

Nonclassicality characterization in photon statistics based on binary-response single-photon detection

This article has been downloaded from IOPscience. Please scroll down to see the full text article.

2011 J. Phys. B: At. Mol. Opt. Phys. 44 205502

(<http://iopscience.iop.org/0953-4075/44/20/205502>)

View [the table of contents for this issue](#), or go to the [journal homepage](#) for more

Download details:

IP Address: 218.26.243.164

The article was downloaded on 30/09/2011 at 02:18

Please note that [terms and conditions apply](#).

Nonclassicality characterization in photon statistics based on binary-response single-photon detection

Yanqiang Guo, Rongcan Yang, Gang Li, Pengfei Zhang, Yuchi Zhang,
Junmin Wang and Tiancai Zhang

State Key Laboratory of Quantum Optics and Quantum Optics Devices, Institute of Opto-Electronics,
Shanxi University, Taiyuan 030006, People's Republic of China

E-mail: tczhang@sxu.edu.cn

Received 24 July 2011, in final form 5 September 2011

Published 29 September 2011

Online at stacks.iop.org/JPhysB/44/205502

Abstract

By employing multiple conventional single-photon counting modules (SPCMs), which are binary-response detectors, instead of photon number resolving detectors, the nonclassicality criteria are investigated for various quantum states. The bounds of the criteria are derived from a system based on three or four SPCMs. The overall efficiency and background are both taken into account. The results of experiments with thermal and coherent light agree with the theoretical analysis. Compared with photon number resolving detectors, the use of a Hanbury Brown–Twiss-like scheme with multiple SPCMs is even better for revealing the nonclassicality of the fields, and the efficiency requirements are not so stringent. Some proposals are presented which can improve the detection performance with binary-response SPCMs for different quantum states.

(Some figures in this article are in colour only in the electronic version)

1. Introduction

Nonclassicality of quantum states plays an important role in quantum optics [1], quantum entanglement and quantum discord [2, 3] and has also become an indispensable tool in quantum physics and quantum information science [4]. Many research groups devoted themselves to implementing and applying various nonclassical effects in theory and experiment, such as photon antibunching, quadrature squeezing and photon number squeezing, sub-Poissonian photon statistics, negativity of the Wigner distribution function, etc. Nonclassical states with these quantum properties can be used as the important sources for quantum information processing [5] and quantum metrology [6]. However, the quantitative measure of nonclassicality for quantum fields is still an open question [7] and none of the properties can identify nonclassicality infallibly and rationally. Although there are some commonly accepted formal definitions of nonclassical states, no necessary and sufficient criterion has been proposed that would allow verification of nonclassicality of an optical state. How to quantify directly and easily the variation of

the nonclassicality of quantum fields based on the current technique is an important task [8]. Since the early works of Walls [9] and Mandel [10], analysis of the photon statistics, the most sensitive and very widespread method of optical measurement, has been used to investigate the nonclassicality of optical fields both in theory and experiment. Photon antibunching [11] and sub-Poissonian [12] are well-known nonclassical effects and have been extensively studied.

For an arbitrary unknown optical source, there are some methods in general to determine its photon statistics, depending on the properties of the source. The photon-number resolving detection (PNRD) [13, 14] has been established by some new technologies and devices, such as transition edge sensor (TES) [15], superconducting optical detectors [16], field-effect transistors with quantum dots [17, 18], etc. All of these methods and technologies already point the way to exciting applications [19–21] although their performance is still very much limited by the requisite superconducting conditions and some technical complexity, which are difficult to realize and involve great cost. Other methods include multiplexed detection, either spatial multiplexing [22] or time

multiplexing [23], maximal likelihood algorithms (MLA) [24], variable attenuation method (VAM) [25], optical homodyne detection (HDT) [26] and reconstruction with intensified charge-coupled device cameras (iCCDs) [27]. Each of these methods has its own advantages and disadvantages. The actual measurement will suffer inevitably from the background (including the dark counts) and finite detection efficiency. These imperfections may smear the quantum features. It is still a challenge to find out a relative simple and practical method without the stringent requirements for the experiment to reveal the nonclassical features of the light fields. In 2004, Waks *et al* [14] provided a criterion for nonclassicality based on the photon counts from a photon number discrimination detector and demonstrated experimentally. Several measures of nonclassicality are proven directly for the two-photon number state [28] or twin beams [29] created by the parametric down-conversion process. Compared to other methods, Waks' criterion is more direct and practical. Nevertheless, the visible light photon counter must be cooled down to very low temperature and shielded from background photons [30]. For this reason, the commercial binary response single-photon counting modules (SPCMs) are still the most commonly used detectors in quantum optics and quantum information science [31–33]. People also exploited hybrid photomultipliers endowed with self-consistent calibration [34] and linear response [35] to directly reconstruct the Wigner function and characterize nonclassical continuous-variable states [36]. The search for an effective method to measure nonclassicality with low demands and good performance on experiment has drawn much attention in recent years.

In this paper, we present a criterion for nonclassicality based on Waks' criterion [14]. There are three points which are different from Waks' treatment: (1) we use the usual binary response SPCMs, instead of the PNRD; (2) by re-defining the ratio of Γ , the criterion is valid in an even wider range; (3) both of the background noise and the overall detection efficiency have been taken into account [37, 38]. We have investigated different light fields, from classical thermal and coherent states to quantum Fock states and squeezed vacuum states (SVS). It is remarkable and quite unexpected that the use of multiple SPCMs is even better than that of the PNRD. We show that, by just using three or four SPCMs, even for an imperfect detection system with considerable losses and background dark counts, the nonclassical features of the incident light can still be extracted and verified even with a moderate quantum efficiency of about 50%. We have also tested the criterion with coherent and thermal light experimentally and the results are in good agreement with the theoretical analysis.

In section 2, we discuss the criterion for different quantum states based on our theoretical analysis, but instead of using PNRD, we employ the SPCMs. New important bounds are introduced following our treatment. We have also compared the theoretical results based on a system of a double Hanbury Brown–Twiss-like (HBT-like) [39] scheme consisting of three or four detectors with that of PNRD and it shows that the performance of the measurement for the nonclassicality can be essentially improved. Section 3 is devoted to the experiment with coherent and thermal light and a summary is presented in section 4.

2. Theoretical analyses

We now introduce a generalized measurable criterion defined by the photon probabilities

$$\Gamma = \frac{\sqrt[N]{P_2}}{\sqrt[N]{P_1} + \sqrt[N]{P_2} + \sqrt[N]{P_3}}, \quad (1)$$

where P_n are the probabilities of observing n ($n = 1, 2, 3$) photons in the state and $N \geq 1$ is an integer. In the original criterion given by Waks [14], $N = 1$. The above defined Γ characterizes the photon statistical properties of the light field in general. We can actually prove that the coherent state is positioned at the border between quantum and classical domain and all classical lights are bounded by maximum $\Gamma_{\max,C}$. It is well known that any classical light has a Glauber–Sudarshan P representation that obeys the requirements of a proper distribution [40], and the corresponding photon number distribution can be written as a sum or integral of Poissonian number distributions [41]. For a Poissonian photon number distribution with $P_C(n) = \alpha^n e^{-\alpha}/n!$, the maximum bound is $\Gamma_{\max,C} = [1 + 2^{(1+1/2N)} 3^{(-1/2N)}]^{-1}$ with the mean photon number $\alpha = \sqrt{6}$. Thus, for a Poissonian distribution, $\Gamma \leq \Gamma_{\max,C}$. And for a distribution of Poissonians with $P_C(\phi) = \int P_C(n)\phi d\alpha$, where ϕ is a probability distribution satisfying $\int \phi d\alpha = 1$, we have

$$\begin{aligned} \Gamma(\phi) &= \frac{\sqrt[N]{\int P_C(2)\phi d\alpha}}{\sqrt[N]{\int P_C(1)\phi d\alpha} + \sqrt[N]{\int P_C(2)\phi d\alpha} + \sqrt[N]{\int P_C(3)\phi d\alpha}} \\ &\leq \frac{\int \sqrt[N]{P_C(2)}\phi d\alpha}{\int \sqrt[N]{P_C(2)}\frac{1}{\Gamma}\phi d\alpha} = \Gamma \leq \Gamma_{\max,C}, \end{aligned} \quad (2)$$

where ϕ is non-negative and $P_C(\phi)$ is strictly positive. Thus, any classical light which is constrained to distributions of Poissonian photon statistics cannot violate the criterion. The reason we generalize Waks' criterion is that the ratio defined by (1) may actually enlarge the range of the mean photon number in which the nonclassicality could be extracted when N is greater than 1. Based on equation (1) and a double HBT-like scheme which consists of three or four SPCMs (as depicted schematically in figure 1), we can extract the nonclassical properties of the light.

Let us first consider the scheme with three SPCMs D_i ($i = 1, 3, 4$) and the detector D_2 will not be used at this moment by removing the beam splitter B_2 (dashed frame), as shown in figure 1. Assume that the input state $|\psi\rangle$ has an intrinsic photon distribution $P_{\text{in}}(n)$. We consider an imperfect detection system with an overall detection efficiency η , which includes the optical collection, propagation and quantum efficiencies of the system. All of these imperfections can be simulated as a beam splitter B_0 with a reflection of $1 - \eta$ and transmission of η [7, 37, 42]. In figure 1, B_1 is either 1:2 (for three SPCMs) or 1:1 (for four SPCMs) lossless beam splitter, and B_2 and B_3 are the 1:1 ones. In our analysis, we assume that all the SPCMs have the same efficiency. Actually, the imbalance effects caused by the non-ideal beamsplitting ratios and unbalanced detectors can be dismissed in our system. Supposing the efficiency difference

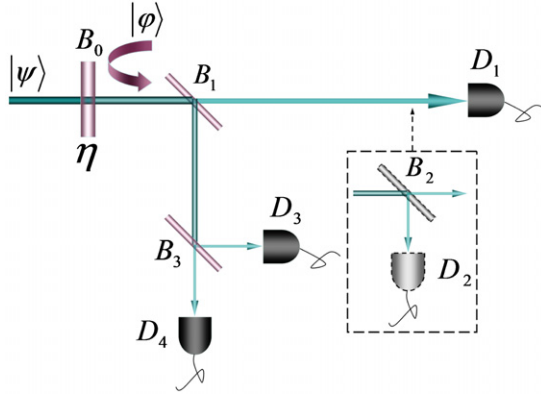


Figure 1. Double HBT-like configuration based on three (without the dashed frame) or four (with the dashed frame) SPCMs with an overall efficiency η and background $|\varphi\rangle$. B_1 is 1:2 (for three SPCMs) or 1:1 (for four SPCMs) lossless beam splitter, and B_2, B_3 are the 1:1 ones. The detector D_2 is not used for a three-detector scheme by removing the beam splitter B_2 (the dashed frame).

of the detectors is $\Delta = \eta_1 - \eta_2$ (or $\eta_3 - \eta_4$), in the usual case of $\eta = 0.5$ and $\Delta = 0.02$ (where η is the total efficiency of the system) the calculated deviation of Mandel's Q factor is about 10^{-5} [43, 44]. In the real system, the unbalance Δ is around 2% and the influence imbalance is negligible.

The photon distribution of the transmitted beam after the B_0 is [1, 45, 46]

$$P_{tr}(m) = \sum_{n=m}^{\infty} P_{in}(n) \frac{n!}{m!(n-m)!} \eta^m (1-\eta)^{(n-m)}, \quad (3)$$

where $P_{in}(n)$ is the photon number distribution of the incident light. The dark counts of the detector and background grey light are both Poissonian which can be simulated as a background light $|\varphi\rangle$ with Poissonian distribution [37] and its weak average number is $\gamma = |\varphi|^2$. The beam mixed with this weak background has a photon number distribution [47]

$$P_{mix}(L) = \sum_{m=0}^L \frac{\gamma^{(L-m)}}{(L-m)!} e^{-\gamma} P_{tr}(m). \quad (4)$$

Here, L is the total number of photon incident on B_1 and if I photons are transmitted, then $L-I$ photons are reflected. These I photons arrive at the detector D_1 and for those $L-I$ photons incident on B_3 there are M photons detected by D_3 and $L-I-M$ by D_4 . The joint probability of detecting I, M and $L-I-M$ photons at D_1, D_3 and D_4 , respectively, can be written as $P(I, M, L-I-M)$. For such a binary response single-photon detector, there is only one count within a response period (including the response time and the dead time) for one or more than one incident photons, so there are totally eight possible photon probabilities:

$$P(1, 1, 1) = \sum_{L=3}^{\infty} P_{mix}(L) \sum_{I=1}^{L-2} \sum_{M=1}^{L-I-1} \left(\frac{1}{3}\right)^L \frac{L!}{I!M!(L-I-M)!}, \quad (5a)$$

$$P(1, 1, 0) = P(1, 0, 1) = P(0, 1, 1) = \sum_{L=2}^{\infty} P_{mix}(L) \sum_{I=1}^{L-1} \left(\frac{1}{3}\right)^L \frac{L!}{I!(L-I)!}, \quad (5b)$$

$$P(1, 0, 0) = P(0, 1, 0) = P(0, 0, 1) = \sum_{L=1}^{\infty} P_{mix}(L) \left(\frac{1}{3}\right)^L, \quad (5c)$$

$$P(0, 0, 0) = P_{mix}(0). \quad (5d)$$

For any specific light source, the ratio given by equation (1) and measured mean photon number are

$$\Gamma_{III} = \frac{\sqrt[3]{P_{III}(2)}}{\sqrt[3]{P_{III}(1)} + \sqrt[3]{P_{III}(2)} + \sqrt[3]{P_{III}(3)}}, \quad (6a)$$

$$\langle n \rangle_{III} = \sum_{n=0}^{\infty} n P(n) = 3P(1, 1, 1) + 2[P(0, 1, 1) + P(1, 1, 0) + P(1, 0, 1)] + [P(1, 0, 0) + P(0, 1, 0) + P(0, 0, 1)] = 3P_{III}(3) + 2P_{III}(2) + P_{III}(1). \quad (6b)$$

Here, $P_{III}(i)$ ($i = 0, 1, 2, 3$) denotes the joint probability of detecting i photons with these three SPCMs.

For an input coherent state $|\alpha\rangle$, the photon distribution is

$$P_{in,C}(n) = \frac{\alpha^n e^{-\alpha}}{n!}, \quad (7)$$

where α is the mean photon number. For a given overall detection efficiency η and background γ , according to equations (3), (4) and (7) we obtain the probability $P_{mix,C}(L)$ of L photons before B_1 :

$$P_{mix,C}(L) = \frac{1}{L!} e^{-(\gamma+\alpha\eta)} (\gamma + \alpha\eta)^L. \quad (8)$$

According to (5) and (6b) the detected photon probabilities and mean photon number are

$$P_{III,C}(3) = e^{-(\gamma+\alpha\eta)} [e^{(\gamma+\alpha\eta)/3} - 1]^3, \quad (9a)$$

$$P_{III,C}(2) = 3 e^{-(\gamma+\alpha\eta)} [e^{(\gamma+\alpha\eta)/3} - 1]^2, \quad (9b)$$

$$P_{III,C}(1) = 3 e^{-(\gamma+\alpha\eta)} [e^{(\gamma+\alpha\eta)/3} - 1], \quad (9c)$$

$$P_{III,C}(0) = e^{-\gamma-\alpha\eta}, \quad (9d)$$

$$\langle n \rangle_{III,C} = 3 - 3 e^{-(\gamma+\alpha\eta)/3}. \quad (9e)$$

Substituting equation (9) into relation (6a), we obtain

$$\Gamma_{III,C} = \frac{\sqrt[3]{P_{III,C}(2)}}{\sqrt[3]{P_{III,C}(1)} + \sqrt[3]{P_{III,C}(2)} + \sqrt[3]{P_{III,C}(3)}} = \frac{\sqrt[3]{3e^{(\gamma+\alpha\eta)/3} - 3}}{\sqrt[3]{(e^{(\gamma+\alpha\eta)/3} - 1)^2} + \sqrt[3]{3e^{(\gamma+\alpha\eta)/3} - 3} + \sqrt[3]{3}}. \quad (10)$$

Equation (10) gives a bound for the coherent light and for any classical Poissonian distributions. If $N = 1$, we have the maximum value of $\Gamma_{III,C}$, which is

$$\Gamma_{III,max,C}^{N=1} = 2\sqrt{3} - 3 \simeq 0.464, \quad (11)$$

with the mean photon number $\alpha_{\max}^{N=1} = \ln(10 + 6\sqrt{3}) \simeq 3.015$ in the ideal case, i.e. $\gamma = 0$, $\eta = 1$. In general, α_{\max}^N depends on the background, the overall efficiency and the number N we choose. From equation (10) we find that the maximum $\Gamma_{\text{III,max,C}} (N \geq 1)$ does not change in the range of $\alpha^N \leq (\alpha_{\max}^N - \gamma)/\eta$. Note that the maximum $\Gamma_{\text{III,max,C}}^N$ gives the bound of a nonclassical criterion based on the three-detector scheme and for any state with $\Gamma_{\text{III}}^N > \Gamma_{\text{III,max,C}}^N$, it is nonclassical.

If the input field is a single-mode thermal state, the photon distribution is a well-known Bose–Einstein distribution:

$$P_{\text{in},T}(n) = \frac{\beta^n}{(1 + \beta)^{n+1}}, \quad (12)$$

where $\beta = [\exp(\hbar\omega/k_B T) - 1]^{-1}$ is the mean photon number. The thermal field shows the bunching effect and super-Poissonian photon distribution. From equations (3), (4) and (12), the probability $P_{\text{mix},T}(L)$ of L photons before the beam splitter B_1 is

$$P_{\text{mix},T}(L) = \sum_{m=0}^L \frac{\gamma^{L-m}}{(L-m)!} e^{-\gamma} \frac{(\beta\eta)^m}{(1 + \beta\eta)^{m+1}}. \quad (13)$$

Similarly, according to equations (5) and (13), we obtain the following ratio for an input thermal state:

$$\begin{aligned} \Gamma_{\text{III},T} &= \frac{\sqrt[N]{P_{\text{III},T}(2)}}{\sqrt[N]{P_{\text{III},T}(1)} + \sqrt[N]{P_{\text{III},T}(2)} + \sqrt[N]{P_{\text{III},T}(3)}} \\ &= \left\{ 1 + \left(\frac{3e^{-\gamma}}{1 + \beta\eta} + \frac{9e^{-\gamma/3}}{3 + \beta\eta} - \frac{18e^{-2\gamma/3}}{3 + 2\beta\eta} \right)^{-\frac{1}{N}} \right. \\ &\quad \times \left[\left(\frac{9e^{-2\gamma/3}}{3 + 2\beta\eta} - \frac{3e^{-\gamma}}{1 + \beta\eta} \right)^{\frac{1}{N}} \right. \\ &\quad \left. \left. + \left(1 - \frac{e^{-\gamma}}{1 + \beta\eta} - \frac{9e^{-\gamma/3}}{3 + \beta\eta} + \frac{9e^{-2\gamma/3}}{3 + 2\beta\eta} \right)^{\frac{1}{N}} \right] \right\}^{-1}. \quad (14) \end{aligned}$$

It is easy to prove from equation (14) that $\Gamma_{\text{III,max,T}}^{N=1} \leq \Gamma_{\text{III,max,C}}^{N=1} = 2\sqrt{3} - 3$ for any background and efficiency. Actually, $\Gamma_{\text{III,max,T}}^{N=1} = 6 - 4\sqrt{2}$ at $\beta_{\text{III,max,T}}^{N=1} = \frac{3}{\sqrt{2}}$ in the ideal case of $\gamma = 0$, $\eta = 1$. Moreover, the bound can be extended to $\Gamma_{\text{III,max,T}}^N \leq \Gamma_{\text{III,max,C}}^N$ for $N > 1$.

The SVS is a typical nonclassical state although its photon distribution can show super-Poissonian with Mandel's Q factor greater than 0. A single-mode SVS can be written as $|\xi\rangle = \hat{S}(\xi)|0\rangle$. Here, the squeezing operator $\hat{S}(\xi) = \exp(\xi^* \hat{a}^2/2 - \xi \hat{a}^{+2}/2)$, $\xi = r \exp(i\theta)$ and $r = |\xi|$ is the squeezing parameter. The photon number distribution of the SVS can be expressed as [48]

$$P_{\text{in,SVS}}(2n) = \frac{[\tanh(r)]^{2n} (2n)!}{\cosh(r) (n! 2^n)^2}, \quad (15)$$

where the mean photon number $\langle n_{\text{SVS}} \rangle = \sinh^2(r)$.

Similarly, we have

$$\begin{aligned} P_{\text{mix,SVS}}(L) &= \sum_{m=0}^L \frac{\gamma^{(L-2m)} \eta^{2m} (2m)! F[\frac{1}{2}+m, \frac{1}{2}+m, \frac{1}{2}; (\eta-1)^2 \tanh^2(r)]}{(L-2m)! e^\gamma (2^m m!)^2 \text{Sech}^{-1}(r) \tanh^{-2m}(r)}, \quad (16) \end{aligned}$$

where $F(a, b, c; z) = \sum_{k=0}^{\infty} \frac{(a)_k (b)_k}{(c)_k} \frac{z^k}{k!}$ is the hypergeometric function.

In figure 2, we plot the ratio Γ_{III} as the functions of the mean photon number (figure 2(a)) and the overall efficiency (figure 2(b)) according to equations (10), (14) and (16) for the coherent state (black solid curves), thermal state (red dashed curves) and SVS (blue dash-dotted curves), respectively. Without loss of generality, we have chosen $N = 1$ and $N = 5$ for comparison. Here, we have used the general specifications of the commercial SPCM (Model SPCM-AQRH-15-FC from PerkinElmer) with a quantum efficiency of about $\eta = 0.5$ at 852 nm and a usual background of $\gamma = 0.01$. It shows that the bound $\Gamma_{\text{III,max,C}}$ cannot be broken for coherent and thermal states, but this bound is broken for the SVS. In figure 2(b), we have shown how Γ_{III} varies along with the overall efficiency for certain background and mean photon number ($\gamma = 0.01$, $\alpha = 10$). The bounds are $\Gamma_{\text{III,max,C}}^{N=1} = 2\sqrt{3} - 3 \simeq 0.464$ and $\Gamma_{\text{III,max,C}}^{N=5} = \frac{10\sqrt{3}}{10\sqrt{3}+2} \simeq 0.358$ with the corresponding mean photon number $\alpha_{\text{III,max}} = 3 \ln(1 + \sqrt{3})$. Again, both the coherent and thermal states are bounded by $\Gamma_{\text{III,max,C}}$ but the classical bound can be broken for the SVS even for low efficiencies around 10%. The breaking of bound $\Gamma_{\text{III,max,C}}$ confirms the nonclassicality of the SVS. For a squeezing of 10 dB [49] and a background of 0.01 the required efficiency is about 24%, which is available for commercial SPCMs [38]. By using the ratio with $N > 1$, the region of the mean photon number over which the bound can be broken is obviously broadened, and the requirements for detection efficiency and incident power are lowered. As shown in figure 2(a), the nonclassical region of the mean photon number is from 0.03 to 4.68 for $N = 5$, but it is from 0.19 to 4.22 for $N = 1$. The result also shows that the larger the number of N , the smaller the depth the bound to be broken.

The Fock state is another typical quantum state which can be utilized in ultra-high sensitive measurement [6, 50] and linear-optics quantum computation [51] and now there are many proposals to generate Fock states with a large number of photons [52, 53]. The measurement of the Fock state with a large number of photons is a challenge. If the input field is a Fock state $|n\rangle$, we have $P_{\text{in},F}(n) = 1$ ($n \geq 1$). Considering the total detection efficiency and the background, the photon number distribution can be written as

$$P_{\text{mix},F}(L) = \sum_{m=0}^L \frac{\gamma^{(L-m)} n!}{(L-m)! m! (n-m)!} e^{-\gamma} \eta^m (1-\eta)^{n-m}. \quad (17)$$

By using equations (5) and (17), similarly, we can find the ratio $\Gamma_{\text{III},F}$ for Fock states

$$\begin{aligned} \Gamma_{\text{III},F} &= \frac{\sqrt[N]{P_{\text{III},F}(2)}}{\sqrt[N]{P_{\text{III},F}(1)} + \sqrt[N]{P_{\text{III},F}(2)} + \sqrt[N]{P_{\text{III},F}(3)}} \\ &= \left[\frac{\sqrt[N]{3e^{-2\gamma/3}(1-2\eta/3)^n - 3e^{-\gamma}(1-\eta)^n}}{\sqrt[N]{3e^{-\gamma}(1-\eta)^n - 6e^{-2\gamma/3}(1-2\eta/3)^n + 3e^{-\gamma/3}(1-\eta/3)^n}} \right. \\ &\quad \left. + \sqrt[N]{1 - e^{-\gamma}(1-\eta)^n + 3e^{-2\gamma/3}(1-2\eta/3)^n - 3e^{-\gamma/3}(1-\eta/3)^n} + 1 \right]^{-1}. \quad (18) \end{aligned}$$

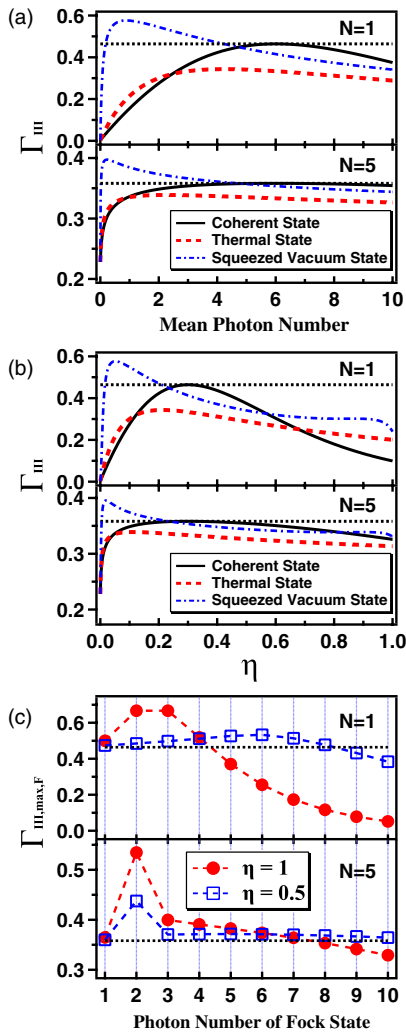


Figure 2. Theoretical analysis based on three SPCMs for $N = 1$ (upper) and $N = 5$ (lower): (a) Γ_{III} versus mean photon number for various states ($\eta = 0.5$ and $\gamma = 0.01$). (b) Γ_{III} as a function of overall efficiency for various states ($\gamma = 0.01$ and the mean photon number is 10). Black dotted line: the classical bound; black solid curve: coherent state; red dashed curve: thermal state; blue dash-dotted curve: squeezed vacuum state. (c) Maximum value $\Gamma_{III,max,F}$ versus photon number of the Fock state with efficiencies $\eta = 1$ (solid circles) and $\eta = 0.5$ (open squares).

For a perfect system with $\eta = 1$, and $\gamma = 0$, the criterion presented here is valid except for $n = 1$, for which $\Gamma_{III,max,F}^{N=1} |_{n=1} = 0$. But this does not mean that the nonclassical features of the Fock states, for example, the well-known single-photon state $|1\rangle$, cannot be extracted with our system. Actually, by mixing the Fock states with the Poissonian background light, the bound can be broken. For example, we can easily obtain $\Gamma_{III,max,F}^{N=1} |_{n=1} = 1/2$ with $\gamma = 3 \ln(2)$, which certainly breaks the classical bound given by equation (11). In figure 2(c), we have given the maximum $\Gamma_{III,max,F}$ as a function of photon numbers, again, for $N = 1$ and 5. It shows that for different efficiencies ($\eta = 1$ and $\eta = 0.5$) $\Gamma_{III,max,F}$ can break the bound of $\Gamma_{III,max,C}$, which proves the nonclassicality extraction of the Fock states. In general, the higher the overall efficiency, the deeper the bound is broken. By choosing a larger N , one can again reduce

the demands on detection efficiency and broaden the region of the photon number over which the ratio is beyond the classical bound. For a given single-photon state and the overall efficiency of $\eta = 0.5$, the ratio is $\Gamma_{III,max,F}^{N=5} |_{n=1} \approx 0.36$ with a background of $\gamma \approx 2.36$, which is beyond the bound.

The above analysis can be extended to the double HBT configuration with a total of four SPCMs by just inserting one more beam splitter and detector (see the dashed frame in figure 1). The treatment is similar to the above. For I photons arriving at the beam splitter B_2 there are K photons detected by D_1 and $I-K$ by D_2 . In this case, there are total 16 probabilities. The new classical bounds for this double-HBT scheme can be obtained. In the case of $N = 1$, we have $\Gamma_{IV,max,C}^{N=1} = 3/7$ with $\alpha = 4 \ln(2)$ for the ideal measurement ($\gamma = 0$, $\eta = 1$). Let us again consider the actual experimental situation with $\gamma = 0.01$, $\eta = 0.5$ and compare the results (here we focus on $N = 1$, and the results are similar for $N > 1$) with the previous scheme by PNRD [14] and the three-detector scheme discussed above. The results are shown in figure 3. It shows the ratio Γ versus the mean photon number for a coherent state (figure 3(a)), thermal state (figure 3(b)) and SVS (figure 3(c)), respectively. Figure 3(d) shows the maximum $\Gamma_{F,max}$ for the Fock state as a function of photon number (in this case the total efficiency is assumed to be 0.5). For these three cases, the corresponding classical bounds are different. For PNRD, the bound is $\Gamma^{N=1} = \frac{\sqrt{6}}{4+\sqrt{6}} \approx 0.38$, while for the schemes with three and four binary-response photon detectors, the bounds are $\Gamma_{III}^{N=1} \approx 0.464$ and $\Gamma_{IV}^{N=1} = 3/7 \approx 0.429$, respectively. All of these bounds could be used to qualify the nonclassical photon statistics. It is clear that for coherent and thermal states, whatever the situations are, the bounds cannot be broken. In the case of $\gamma = 0.01$, $\eta = 0.5$ as shown in figure 3(c), it should be noted that for the SVS, with four SPCMs, the bound can be broken when the squeezing is higher than 2.81 dB. The maximum value appears at a squeezing of about 7 dB, corresponding to $\langle n_{svs} \rangle \approx 0.8$, for an efficiency of 50% and a background of 0.01. Even if the efficiency is as low as 20%, the bound can still be broken for the present best SVS with 12.7 dB [54] and a background of 0.01. In the scheme of PNRD, as shown by Waks *et al*, the overall efficiency must be higher than $\eta \approx 0.55$ in order to break the corresponding bound [14]. For the Fock state (see figure 3(d)), the bounds can be broken for all of the three cases discussed above. In the three- or four-SPCM scheme, the photon number range for which the bound is broken is wider than that of the PNRD scheme. This implies that the requirement for detection efficiency based on the system of multiple binary response photon detectors is much lower than that of the PNRD. All of this suggests that, based on the multiple binary-response photon detector system, one can directly measure the nonclassicality of photon statistics with good performance and low requirements for detection efficiency.

3. Experiment

Since right now we have no squeezed light at the wavelength for our SPCMs, we have tested the about discussion by

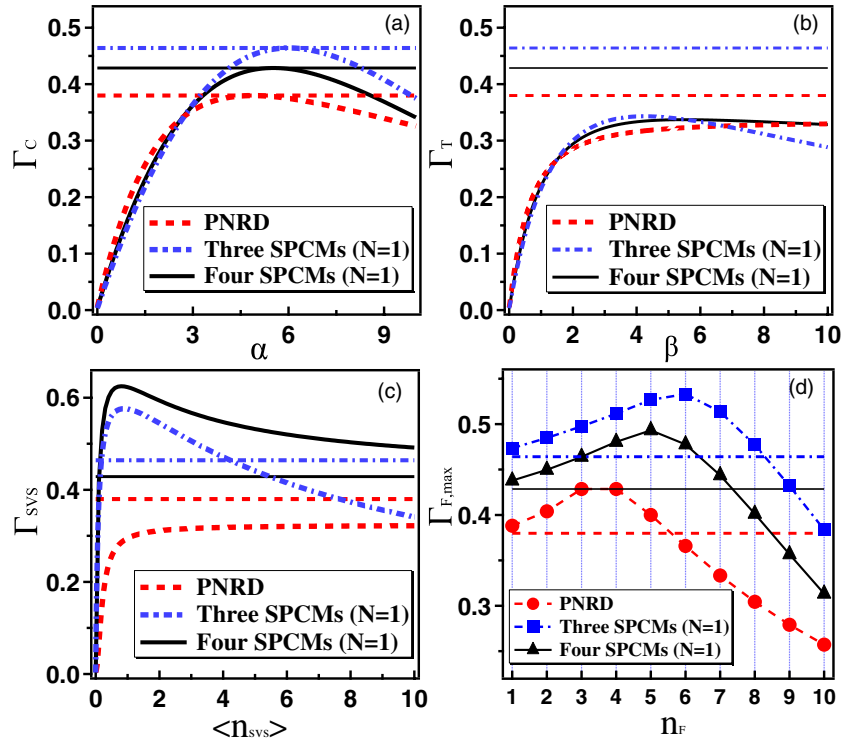


Figure 3. Ratio of Γ as a function of mean photon number for $N = 1$, based on the double HBT scheme (black solid curves), three-SPCM scheme (blue dash-dotted curves) and PNRD scheme (red dashed curves) for different light fields: (a) coherent state, (b) thermal state, (c) squeezed vacuum state and (d) Fock state ($\eta = 0.5$). We have chosen $\gamma = 0.01$, $\eta = 0.5$ in (a), (b) and (c). The corresponding bounds (horizontal line) for the three schemes are also shown.

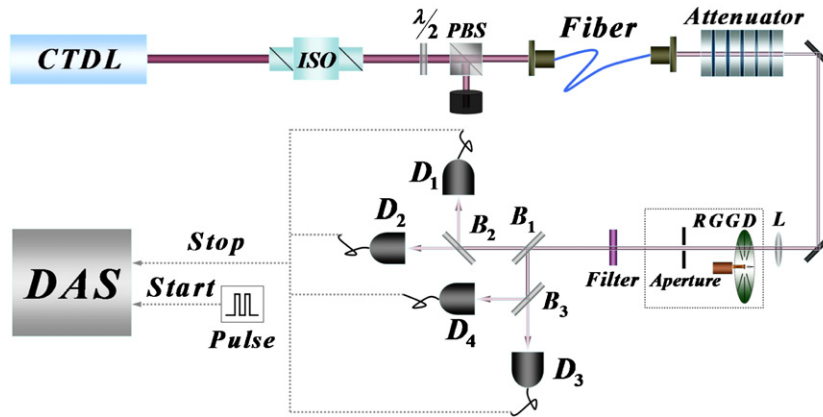


Figure 4. Schematic of the experimental setup. CTDL: continuously tunable diode laser. ISO: Isolator. RGGD: rotating ground glass disk. B_i ($i = 1, 2, 3$): beam splitters. D_i ($i = 1, 2, 3, 4$): single-photon-counting modules, SPCMs. DAS: data acquisition system. $\lambda/2$: half-wave plate. PBS: polarized beam splitter. L : optical lens.

measuring the ratio Γ experimentally based on the four-SPCM scheme for various mean photon numbers of the coherent and thermal states. The experiment setup is shown in figure 4. A continuously tunable diode laser operating in a single longitudinal mode at 852 nm is used as the laser source. The beam goes through an optical isolator. A half-wave plate and a polarized beam splitter (PBS) are used to control the intensity. The beam is coupled into a single-mode fiber which is used as a spatial filter. After an attenuator, the beam enters into a pseudo-thermal light generation system [55] (shown inside the dashed box in figure 4), which consists

of a rotating ground glass disc and an aperture. The light power is controlled so that the photon counting rate is below 3×10^6 counts s^{-1} , which is the maximum allowed counting rate of each SPCM. B_1, B_2, B_3 are 1:1 beam splitters. The photons eventually arrive at four SPCMs: D_1, D_2, D_3 and D_4 (SPCM-AQR-15, PerkinElmer Optoelectronics). The quantum efficiency of the module is $49\% \pm 1\%$ at 852 nm and the dark count is about 90 counts s^{-1} . The background of the system γ is about 0.01. The outputs of the SPCMs go to a data acquisition system (P7888, Fastcomtec GmbH). The detector and the data card are triggered together by a

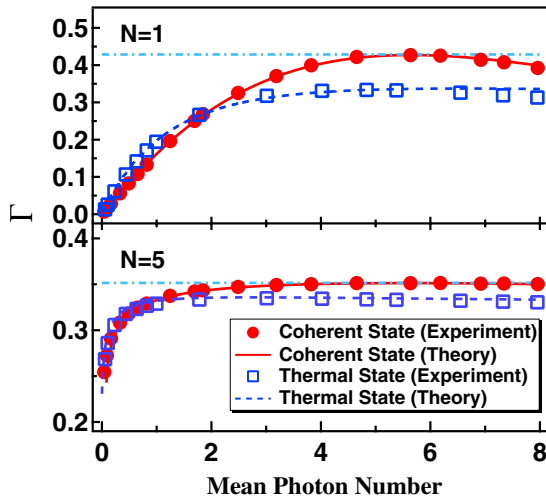


Figure 5. The measured ratio Γ for coherent (red solid circles) and thermal light (blue open squares) versus the mean photon number, based on the four-SPCM scheme ($N = 1, 5$). The red solid and blue dashed curves are theoretical fittings.

pulse generator, and the photon count statistical analysis is performed. The value of N ($N = 1, 5$) is modified by different data processings with the same experiment setup. The results ($N = 1, 5$) are shown in figure 5. The total acquisition time is 1 s. $P_{IV}(i)$ ($i = 0, 1, 2, 3, 4$) is extracted from the probability of registering i clicks (i.e. the coincidence of clicking i detectors) in the acquisition time. The detectors are used in the 3 ns coincidence window. The response period (including the response time and the following dead time) is 55 ns. We change the count rate from 5×10^3 to 3×10^6 counts s^{-1} by changing the incident power. The red solid circles are the experimental data for coherent light while the blue open squares are for thermal light. The error bars are too small to be seen. The solid and dashed curves are the theoretical fittings based on the above analysis.

Clearly, we can see that the measured Γ for the coherent and thermal beams are bounded by $\Gamma_{IV,max,C}^{N=1} = 3/7$ and $\Gamma_{IV,max,C}^{N=5} \simeq 0.352$, respectively. The results agree with the theoretical prediction very well for both the coherent and thermal states. In fitting the experimental results we have considered that the input light is not pure thermal or coherent states, but a mixture of thermal and coherent light [37, 56, 57]. The proportion is mainly determined by the rotating ground glass system and the background of the environment [57–59]. When the input light is a coherent field, the mixed model allows one to consider the coherent part as a signal and a small thermal part as random Gaussian noise. Thus, the probability distribution of the input field is [56]

$$P_{in,Mix}(n) = \frac{\beta^n}{(1 + \beta)^{n+1}} \exp\left(\frac{-\alpha}{\beta + 1}\right) \times \left[{}_1F_1\left(-n; 1; \frac{-\alpha}{\beta^2 + \beta}\right) \right], \quad (19)$$

where ${}_1F_1$ is a confluent hypergeometric function. α and β are the mean photon number of coherent and thermal light, respectively. Based on equation (19) the best fittings

between the theoretical analysis and the experiment results are obtained and shown in figure 5. The red curve is for the coherent light with 0.3% of thermal light mixed in. The measured mean photon number corresponding to the maximum $\Gamma_{max,C}$ is 5.64 ± 0.01 , which is in accordance with the theoretical prediction 5.63 based on the present efficiency and background. The blue dashed curve corresponds to the thermal light with 1% of coherent light mixed in. In both cases, the theoretical results are in good agreement with the experimental data. In addition, the detector efficiency of $49\% \pm 1\%$ has been taken into account. The maximum counting rate of the detector prevents the system from reaching a relatively high mean photon number. There is still a minor discrepancy between the theory and experiment for thermal light, especially at high counting rate. This may be due to the saturation of multi-photon counting of the detectors for thermal light at relative intense light.

4. Conclusion

In conclusion, we have presented a nonclassicality criterion for photon statistics based on multiple binary-response photon detectors, and have compared the result with that of the PNRD. It is shown that even without PNRD, the nonclassicality can still be measured directly by photon countings based on either three or four SPCMs. The bound of $\Gamma_{III} \simeq 0.476$ for three binary photon detectors and $\Gamma_{IV} = 3/7$ for four detectors are obtained. Moreover, the requirement for the overall efficiency is less stringent. We have performed experiments based on the four-SPCM scheme with coherent and thermal light and verified the bound. The results are in good agreement with the theoretical analysis. These new bounds of nonclassicality could be used as a test for the quantum features of the light. Because of the comparative simplicity of the setup, it is feasible to implement this scheme in quantum information processing.

Acknowledgments

The authors acknowledge the support from the Natural Science Foundation of China (grants nos 10974125, 60808006, 60821004, 61078051 and 11125421) and the 973 program (2012CB921601).

References

- [1] Mandel L and Wolf E 1995 *Optical Coherence and Quantum Optics* (Cambridge: Cambridge University Press)
- [2] Scully M O and Zubairy M S 1997 *Quantum Optics* (Cambridge: Cambridge University Press)
- [3] Ollivier H and Zurek W H 2001 *Phys. Rev. Lett.* **88** 017901
- [4] Datta A and Gharibian S 2009 *Phys. Rev. A* **79** 042325
- [5] Bouwmeester D, Ekert A K and Zeilinger A 2000 *The Physics of Quantum Information* (Berlin: Springer)
- [6] Cirac J I, Zoller P, Kimble H J and Mabuchi H 1997 *Phys. Rev. Lett.* **78** 3221
- [7] Banaszek K, Demkowicz-Dobrzanski R and Walmsley I A 2009 *Nat. Photon.* **3** 673
- [8] Li J, Li G, Wang J M, Zhu S Y and Zhang T C 2010 *J. Phys. B: At. Mol. Opt. Phys.* **43** 085504
- [9] Li S B, Zou X B and Guo G C 2007 *Phys. Rev. A* **75** 045801

- [9] Carmichael H J and Walls D F 1976 *J. Phys. B: At. Mol. Phys.* **9** L43
Carmichael H J and Walls D F 1976 *J. Phys. B: At. Mol. Phys.* **9** 1199
- [10] Kimble H J, Dagenais M and Mandel L 1977 *Phys. Rev. Lett.* **39** 691
Mandel L 1979 *Opt. Lett.* **4** 205
- [11] Paul H 1982 *Rev. Mod. Phys.* **54** 1061
- [12] Machida S and Yamamoto Y 1986 *IEEE J. Quantum Electron.* **QE-22** 617
Breitenbach G, Müller T, Pereira S F, Poizat J-Ph, Schiller S and Mlynek J 1995 *J. Opt. Soc. Am. B* **12** 2304
- [13] Smithy D T, Beck M, Raymer M G and Faridani A 1993 *Phys. Rev. Lett.* **70** 1244
- [14] Waks E, Diamanti E, Sanders B C, Bartlett S D and Yamamoto Y 2004 *Phys. Rev. Lett.* **92** 113602
- [15] Lita A E, Miller A J and Nam S W 2008 *Opt. Express* **16** 3032
- [16] Miller A J, Nam S W, Martinis J M and Sergienko A V 2003 *Appl. Phys. Lett.* **83** 791
Schuster D I et al 2007 *Nature* **445** 515
- [17] Shields A J, O'Sullivan M P, Farrer I, Ritchie D A, Hogg R A, Leadbeater M L, Norman C E and Pepper M 2000 *Appl. Phys. Lett.* **76** 3673
- [18] Rowe M A, Gansen E J, Greene M, Hadfield R H, Harvey T E, Su M Y, Nam S W, Mirin R P and Rosenberg D 2006 *Appl. Phys. Lett.* **89** 253505
- [19] Verevkin A, Zhang J, Sobolewski R, Lipatov A, Okunev O, Chulkova G, Korneev A, Smirnov K, Gol'tsman G N and Semenov A 2002 *Appl. Phys. Lett.* **80** 4687
- [20] Di Giuseppe G, Atatüre M, Shaw M D, Sergienko A V, Saleh B E A, Teich M C, Miller A J, Nam S W and Martinis J 2003 *Phys. Rev. A* **68** 063817
- [21] Takesue H, Nam S W, Zhang Q, Hadfield R H, Honjo T, Tamaki K and Yamamoto Y 2007 *Nat. Photon.* **1** 343
Rosenberg D, Harrington J W, Rice P R, Hiskett P A, Peterson C G, Hughes R J, Lita A E, Nam S W and Nordholt J E 2007 *Phys. Rev. Lett.* **98** 010503
- [22] Jiang L A, Dauler E A and Chang J T 2007 *Phys. Rev. A* **75** 062325
Divochiy A et al 2008 *Nat. Photon.* **2** 302
- [23] Achilles D, Silberhorn C, Śliwa C, Banaszek K and Walmsley I A 2003 *Opt. Lett.* **28** 2387
Banaszek K and Walmsley I A 2003 *Opt. Lett.* **28** 52
Fitch M J, Jacobs B C, Pittman T B and Franson J D 2003 *Phys. Rev. A* **68** 043814
- [24] Zavatta A, Viciani S and Bellini M 2004 *Science* **306** 660
Zambra G, Andreoni A, Bondani M, Gramegna M, Genovese M, Brida G, Rossi A and Paris M G A 2005 *Phys. Rev. Lett.* **95** 063602
Hradil Z, Mogilevtsev D and Řeháček J 2006 *Phys. Rev. Lett.* **96** 230401
- [25] Zhang S L, Zou X B, Li C F, Jin C H and Guo G C 2009 *Phys. Rev. A* **80** 043807
- [26] Lvovsky A I, Hansen H, Aichele T, Benson O, Mlynek J and Schiller S 2001 *Phys. Rev. Lett.* **87** 050402
- Munroe M, Boggavarapu D, Anderson M E and Raymer M G 1995 *Phys. Rev. A* **52** R924
- [27] Haderka O, Peřina J Jr, Hamar M and Peřina J 2005 *Phys. Rev. A* **71** 033815
Hamar M, Peřina J Jr, Haderka O and Michálek V 2010 *Phys. Rev. A* **81** 043827
- [28] Achilles D, Silberhorn C and Walmsley I A 2006 *Phys. Rev. Lett.* **97** 043602
- [29] Waks E, Sanders B C, Diamanti E and Yamamoto Y 2006 *Phys. Rev. A* **73** 033814
- [30] Takeuchi S, Kim J, Yamamoto Y and Hogue H H 1999 *Appl. Phys. Lett.* **74** 1063
- [31] Hong C K, Ou Z Y and Mandel L 1987 *Phys. Rev. Lett.* **59** 2044
- [32] Bouwmeester D, Pan J W, Mattle K, Eibl M, Weinfurter H and Zeilinger A 1997 *Nature* **390** 575
- [33] Hadfield R H 2009 *Nat. Photon.* **3** 696
- [34] Ramilli M, Allevi A, Chmill V, Bondani M, Caccia M and Andreoni A 2010 *J. Opt. Soc. Am. B* **27** 852
- [35] Andreoni A and Bondani M 2009 *Phys. Rev. A* **80** 013819
- [36] Bondani M, Allevi A and Andreoni A 2009 *Opt. Lett.* **34** 1444
- [37] Li G, Zhang T C, Li Y and Wang J M 2005 *Phys. Rev. A* **71** 023807
- [38] Li Y, Li G, Zhang Y C, Wang X Y, Zhang J, Wang J M and Zhang T C 2007 *Phys. Rev. A* **76** 013829
- [39] Hanbury Brown R and Twiss R Q 1956 *Nature* **178** 1046
- [40] Wang T Y and Xiao L T 2006 *J. Appl. Opt.* **27** 281
- [41] Sanders B C, Bartlett S D, Rudolph T and Knight P L 2003 *Phys. Rev. A* **68** 042329
- [42] Spagnolo N, Vitelli C, De Angelis T, Sciarrino F and De Martini F 2009 *Phys. Rev. A* **80** 032318
- [43] Kok P and Braunstein S L 2001 *Phys. Rev. A* **63** 033812
- [44] Wang T Y and Xiao L T 2006 *J. Appl. Opt.* **27** 281
- [45] Lee C T 1993 *Phys. Rev. A* **48** 2285
- [46] Kiss T, Herzog U and Leonhardt U 1995 *Phys. Rev. A* **52** 2433
- [47] Abate J A, Kimble H J and Mandel L 1976 *Phys. Rev. A* **14** 788
- [48] Bachor H A 1998 *A Guide to Experiments in Quantum Optics* (Germany: Wiley-VCH)
- [49] Vahlbruch H, Mehmet M, Chelkowski S, Hage B, Franzen A, Lastzka N, Goßler S, Danzmann K and Schnabel R 2008 *Phys. Rev. Lett.* **100** 033602
- [50] Wildfeuer C F, Pearlman A J, Chen J, Fan J Y, Migdall A and Dowling J P 2009 *Phys. Rev. A* **80** 043822
- [51] Knill E, Laflamme R and Milburn G J 2001 *Nature* **409** 46
- [52] Brown K R, Dani K M, Stamper-Kurn D M and Whaley K B 2003 *Phys. Rev. A* **67** 043818
- [53] Varcoe B T H, Brattke S and Walther S 2004 *New J. Phys.* **6** 97
- [54] Eberle T, Steinlechner S, Bauchrowitz J, Händchen V, Vahlbruch H, Mehmet M, Müller-Ebhardt H and Schnabel R 2010 *Phys. Rev. Lett.* **104** 251102
- [55] Basano L and Ottonello P 1982 *Am. J. Phys.* **50** 996
- [56] Lachs G 1965 *Phys. Rev.* **138** B1012
- [57] Li Y, Zhang Y C, Zhang P F, Guo Y Q, Li G, Wang J M and Zhang T C 2009 *Chin. Phys. Lett.* **26** 074205
- [58] Arecchi F T 1965 *Phys. Rev. Lett.* **15** 912
- [59] Asakura T 1970 *Opto-Electron.* **2** 115